A Nonlinear Admittance-based Holomorphic Embedding Method for Power Flow Calculation

Yongjian Luo, Chengxi Liu, Zaiyu He, Pengfei Tang, Jiangbei Han
School of Electrical Engineering and Automation
Wuhan University
Wuhan, China
yongjianluo@whu.edu.cn; liuchengxi@whu.edu.cn; hezaiyu@whu.edu.cn; tangpengfei@whu.edu.cn; hanjiangbei@whu.edu.cn

***Abstract*—This paper proposes a nonlinear admittance-based holomorphic embedding method (NLA-HEM) for power flow calculation with enhanced convergence performance. The proposed method first decomposes the admittance matrix into symmetric and asymmetric components and constructs a holomorphic embedding formulation with parameter-controlled admittance integration. A tun-able embedding path is designed to progressively incorporate asymmetric elements, ensuring numerical stability throughout the solution process. Case studies on the 1888-bus system and other benchmark systems demonstrate that the proposed method achieves improved convergence robustness compared to classical holomorphic embedding method (C-HEM), especially under ill-conditioned and large-scale scenarios. The results verify that NLA-HEM not only overcomes known convergence limitations of existing methods but also provides a diagnosable and adaptable framework for reliable power flow solutions.**

Index Terms—Holomorphic embedding method, nonlinear admittance embedding, power flow calculation, convergence improvement, convergence diagnosis.

I. Introduction

Power flow calculation serves as the fundamental tool for power system analysis, operation, and planning. Since its inception, a variety of numerical methods have been developed to solve the nonlinear power flow equations. Among these, the Newton-Raphson (NR) method and its variants have long been established as the industry standard due to their quadratic convergence characteristics[1]. These conventional methods, while powerful, inherently face challenges in achieving convergence for ill-conditioned systems, which has motivated the exploration of more robust methods.

In recent years, the Classical Holomorphic Embedding Method (C-HEM) has emerged as a promising approach for power flow, renowned for its theoretical guarantee of convergence to the correct operational solution[2]. This property has attracted considerable research attention and has led to its application in various scenarios, including distribution system power flow analysis[3], hybrid AC/DC power system analysis[4], and uncertainty-oriented probabilistic power flow computation[5], voltage stability analysis[6],[7], and etc. Compared with conventional iterative algorithms, HEM provides a theoretically grounded alternative framework for solving power flow problems.

However, subsequent studies have revealed that the practical convergence performance of HEM is highly sensitive to its specific embedding formulation. Contrary to the theoretical guarantees, convergence issues have been documented in challenging cases, such as the 1888-bus system and 6468-bus system in the MATPOWER toolkit[8]. These failures are often attributed to numerical instability arising from the inherent ill-condition of the system, or an improperly designed embedding path that leads to singularities or branch points before reaching the physical solution at s=1. To address these issues, several improved HE formulation has been developed. In [9], a restarted HE formulation is proposed utilizing Padé approximants with very low orders. In [10], a fast and flexible HE method using good initial germ solution is proposed. In these methods, can be considered methods for adopting a good initial guess, however, selecting a promising initial guess remains a sophisticated issue.

In this paper, we propose an enhanced holomorphic embedding method for power flow calculation, termed the nonlinear admittance-based HEM (NLA-HEM). The main contributions of this work are summarized as follows:

1) A novel holomorphic embedding formulation is established through a nonlinear decomposition of the admittance matrix.

2) A parameter-controlled embedding path is designed to gradually incorporate asymmetric admittance components, providing a tunable mechanism to ensure numerical stability throughout the solution process.

3) Comprehensive case studies on the 1888-bus system and other test cases demonstrate the superior performance of the proposed method in both convergence reliability and operational diagnostics compared to conventional algorithms.

This work was supported by Smart Grid-National Science and Technology Major Project (2025ZD0806501)

979-8-3315-8138-1

The remainder of this paper is organized as follows. Section II introduces the C-HEM and its mathematical formulation. Section III presents the proposed nonlinear admittance-based framework and derives the corresponding holomorphic embedding formulation based on the decomposed matrix structure. Section IV details the numerical solution procedure of the NLA-HEM, including the recursive coefficient calculation and the embedded convergence detection mechanism. In Section V, case studies on the 1888-bus system and other test systems are carried out to validate the convergence performance and robustness of the proposed method. Section VI summarizes the main conclusions.

II. Power Flow Equations And Formulation Of C-HEM

For a N_b-bus power system, which includes PQ bus, and PV nodes and slack bus, the AC power flow equations for these three types of buses in the rectangular coordinate system are given by (1) to (3).

$$\sum_{j=1}^{N_b} Y_{ij} V_j = \frac{S_i^*}{V_i^*}, \forall i \in \Omega^{\mathrm{PQ}} \tag{1}$$

$$\begin{cases} P_i = \Re(V_i \sum_{j=1}^{N_b} Y_{ij}^* V_j^*) \\ |V_i| = U_i^{\mathrm{sp}} \end{cases}, \forall i \in \Omega^{\mathrm{PV}} \tag{2}$$

$$V_i = U_i^{\mathrm{sp}}, \forall i \in \Omega^{\mathrm{SL}} \tag{3}$$

where the sets of PQ, PV and slack bus are denoted as Ω^{PQ}, Ω^{PV} and Ω^{SL}; respectively; Y_{ij} is admittance matrix element corresponding to the connection between bus i and bus j; V_i and V_j are the complex voltages at bus i and j, respectively; S_i, P_i and Q_i represent the apparent, active and reactive power injection at bus i, respectively; U_i^{sp} is the specified voltage magnitude of PV buses and slack bus; $(z)^*$, $\Re(z)$ and $|z|$ represents the conjugate, real part, and absolute value operators, respectively.

The holomorphic embedding formulation of the C-HEM is given in (4)-(6). The embedded form of PQ buses is given by (4). The embedded form of PV buses is given by (5). The embedded form of slack bus is given by (6).

$$\sum_{j=1}^{N_b} Y_{ij}^{\mathrm{tr}} V_j(s) = \frac{sS_i^*}{V_i^*(s^*)} - sY_i^{\mathrm{sh}} V_i(s), \forall i \in \Omega^{\mathrm{PQ}} \tag{4}$$

$$\begin{cases} \sum_{j=1}^{N_b} Y_{ij}^{\mathrm{tr}} V_k(s) = \dfrac{sP_i - \mathrm{j}Q_i(s)}{V_i^*(s^*)} - sY_i^{\mathrm{sh}} V_i(s) \\ V_i(s) V_i^*(s^*) = 1 + s\left((U_i^{\mathrm{sp}})^2 - 1\right) \end{cases}, \forall i \in \Omega^{\mathrm{PV}} \tag{5}$$

$$V_i(s) = 1 + s(U_i^{\mathrm{sp}} - 1), \forall i \in \Omega^{\mathrm{SL}} \tag{6}$$

where s is the complex embedding parameter; Y_{ij}^{tr} corresponds to the series branch part of the admittance matrix and Y_i^{sh} correspond to the shunt part of the admittance matrix. The detailed mathematical formulation for constructing the matrices for Y_{ij}^{tr} and Y_i^{sh} is presented in (7). For PQ buses, only the complex voltage $V_i(s)$ is constructed as a holomorphic function of s. For PV buses, in addition to the complex voltage, the unknown reactive power injection $Q_i(s)$ is also expressed as an unknown holomorphic function as in (5).

$$Y_{ij}^{\mathrm{tr}} = \begin{cases} -\sum_{\substack{j=1 \\ i \neq j}}^{N_b} Y_{ij}, & i = j \\ Y_{ij}, & i \neq j \end{cases}, \quad Y_i^{\mathrm{sh}} = \begin{cases} Y_{ii} - Y_{ij}^{\mathrm{tr}}, & i = j \\ 0, & i \neq j \end{cases} \tag{7}$$

To address the presence of voltage reciprocal terms on the right-hand side of equations (4)-(5), an auxiliary variable $W_i(s) = 1/V_i(s)$ is introduced and incorporated into the solution process. The detailed solution process of the C-HEM can be found in [11].

III. Formulation Of The Proposed Non-linear Admittance-based Holomorphic Embedding Method

In this section, the formulation of the proposed NLA-HEM is given detailed. The holomorphic embedding formulation for PQ bus, PV bus and slack bus is given by

$$\begin{aligned} \sum_{j=1}^{N_b} Y_{ij}^{\mathrm{sym,tr}} V_j(s) = \frac{sS_i^*}{V_i^*(s^*)} - sY_i^{\mathrm{sym,sh}} V_i(s) \\ -\frac{1}{K} \sum_{k=1}^{K} \sum_{j=1}^{N_b} s^k Y_{ij}^{\mathrm{asy}} V_j(s) \end{aligned}, \forall i \in \Omega^{\mathrm{PQ}} \tag{8}$$

$$\begin{cases} \sum_{j=1}^{N_b} Y_{ij}^{\mathrm{sym,tr}} V_j(s) = \dfrac{sP_i - jQ_i(s)}{V_i^*(s^*)} - sY_i^{\mathrm{sym,sh}} V_i(s) \\ \qquad -\dfrac{1}{K} \sum_{k=1}^{K} \sum_{j=1}^{N_b} s^k Y_{ij}^{\mathrm{asy}} V_j(s) \\ V_i(s) V_i^*(s^*) = 1 + s(U_i^{\mathrm{sp}2} - 1) \end{cases}, \forall i \in \Omega^{\mathrm{PQ}} \tag{9}$$

$$V_i(s) = 1 + s(U_i^{\mathrm{sp}} - 1), \forall i \in \Omega^{\mathrm{SL}} \tag{10}$$

where the matrix $Y_{ij}^{\mathrm{sym,tr}}$, $Y_i^{\mathrm{sym,sh}}$ and Y_{ij}^{uns} represent the symmetric transmission part, the symmetric shunt part, and the asymmetrical part of the admittance matrix, respectively; the parameter K is a positive integer ($K \geq 1$) governing the order or rate of the asymmetrical part's incremental incorporation into the embedding process.

From (8)-(10), it can be shown that the holomorphic embedding formulation recovers to the original power flow equations at s=1. At s=0, (8)-(10) attains a known germ solution as C-HEM.

Fig. 1 illustrates the corresponding admittance matrix structures used in the C-HEM and the proposed NLA-HEM. In NLA-HEM, the admittance matrix $\mathbf{Y}$ is split into the following components: $\mathbf{Y}^{\mathrm{sys,tr}}$, $\mathbf{Y}^{\mathrm{sys,sh}}$, and $\mathrm{Y}^{\mathrm{asy}}$. The symmetric admittance matrix $\mathbf{Y}^{\mathrm{sys}}$ is obtained by setting the transformer tap ratio to 1.0 and the phase shift angle of 0°.

979-8-3315-8138-1

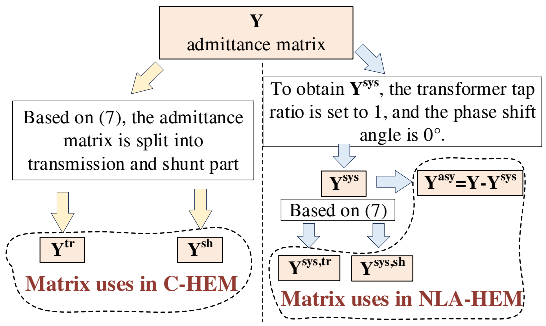

Fig. 1 The admittance matrix splitting diagram.

The proposed method is treated as the nonlinear admittance HEM due to its distinctive treatment of the admittance trajectory in the complex plane.

As illustrated in Fig. 2, both the C-HEM and the proposed NLA-HEM originate from a common initial admittance value at s=0 and progress toward the target physical solution at s=1. While the C-HEM follows a linear admittance path with respect to the embedding parameter s, the proposed NLA-HEM follows a deliberately designed nonlinear trajectory. This nonlinear embedding path enhances numerical stability and facilitates convergence in ill-conditioned systems. This phenomenon can be attributed to the process of gradually introducing the $\mathbf{Y}^{\text{asy}}$ matrix into the system. In certain grid, this incremental addition can affect the numerical conditioning, thereby influencing the convergence behavior. Notably, the large Y^{asy} values induced by phase-shift transformers and their numerical implications are analyzed in detail in our paper [12].

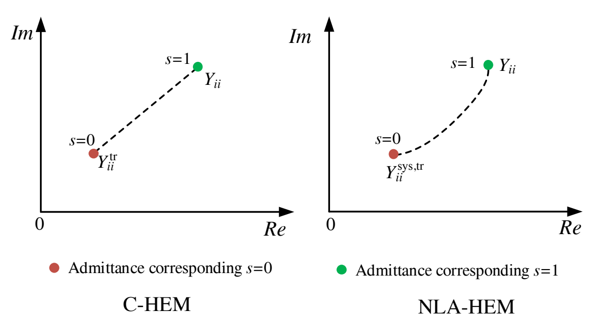

Fig. 2 Admittance trajectories of C-HEM and NLA-HEM in the complex plane.

IV. Solution Process of NLA-HEM

In this section, the formulation of the proposed NLA-HEM is given detailed. The holomorphic embedding formulation for PQ bus, PV bus and slack bus is given by

The unknown voltage, reactive power injection at PV buses and the reciprocal of voltage can be expressed as Maclaurin series of the embedded complex variables shown by (11)-(13).

$$V_i(s)=\sum\nolimits_{n=0}^{\infty}V_i[n]s^n \tag{11}$$

$$Q_i(s)=\sum\nolimits_{n=0}^{\infty}Q_i[n]s^n \tag{12}$$

$$W_i^*(s^*)=\frac{1}{V_i^*(s^*)}=\sum\nolimits_{n=0}^{\infty}W_i^*[n]s^n \tag{13}$$

By substituting the power series defined in (11)-(13) into Eqs. (8)-(10), and equating coefficients of like powers of s on both sides of the equations, a system of linear equations for the power series coefficients at each order can be derived. These resulting equations can be solved recursively to obtain all voltage and power coefficients.

A. *Germ Solution*

The germ solution for the unknown coefficients $V_i[0]$, $W_i[0]$, $Q_i[0]$ can be obtained by solving the equations (14)-(16).

$$\sum\nolimits_{j=1}^{N_b}Y_{ij}^{\text{sym,tr}}V_j[0]=0 \quad ,\forall i\in\Omega^{\text{PQ}} \tag{14}$$

$$\begin{cases}\sum\nolimits_{j=1}^{N_b}Y_{ij}^{\text{sym,tr}}V_j[0]=-jQ_i[0]W_i^*[0] \\ V_i[0]V_i^*[0]=1\end{cases},\forall i\in\Omega^{\text{PQ}} \tag{15}$$

$$V_i[0]V_i^*[0]=U_i^{\text{sp2}},\forall i\in\Omega^{\text{SL}} \tag{16}$$

The solution for $V_i[0]$, $W_i[0]$ and $Q_i[0]$ are straightforwardly derived, as shown in equation (17).

$$\begin{cases}V_i[0]=1,W_i[0]=1,\forall i \\ Q_i[0]=0,\forall i\in\Omega^{\text{PV}}\end{cases} \tag{17}$$

B. *High-Order Power Series*

The high order coefficients $V_i[n]$, $W_i[n]$, $Q_i[n]$can be obtained by solving the recursive equations shown in (18)-(20), which are derived by equating the coefficients on both sides.

$$\sum\nolimits_{j=1}^{N_b}Y_{ij}^{\text{sym,tr}}V_j[n]=S_i^*W_i^*[n-1]-Y_i^{\text{sym,sh}}V_i[n-1]-\Phi,\forall i\in\Omega^{\text{PQ}} \tag{18}$$

$$\begin{cases}\sum\nolimits_{j=1}^{N_b}Y_{ij}^{\text{sym,tr}}V_j[n]+jQ_i[n]=P_iW_i^*[n-1] \\ -j\sum\limits_{d=1}^{n-1}Q_i[d]W_i^*[n-d]-Y_i^{\text{sym,sh}}V_i[n-1]-\Phi[n] \\ V_{i,re}[n]=\delta_{n1}(U_i^{\text{sp2}}-1)-\sum\limits_{d=1}^{n-1}V_i[d]V_i^*[n-d]\end{cases},\forall i\in\Omega^{\text{PV}} \tag{19}$$

$$V_i[n]=\delta_{n1}(U_i^{\text{sp}}-1),\forall i\in\Omega^{\text{SL}} \tag{20}$$

In (20), δ_{n1} equals 1 if n equals 1; otherwise, δ_{n1} equals 0. The right-hand side of (18)-(20) is the low-order power series obtained before the n-th solution. In (18) and (19), the $\Phi[n]$ is given below.

$$\Phi[n]=\begin{cases}\dfrac{1}{K}\sum\limits_{j=1}^{N_b}Y_{ij}^{\text{asy}}V_j[0],n=1 \\ \dfrac{1}{K}\sum\limits_{k=1}^{K}\sum\limits_{j=1}^{N_b}Y_{ij}^{\text{asy}}V_j[n-k]+\dfrac{1}{K}\sum\limits_{j=1}^{N_b}Y_{ij}^{\text{asy}}V_j[0],otherwise \\ \dfrac{1}{K}\sum\limits_{k=1}^{K}\sum\limits_{j=1}^{N_b}Y_{ij}^{\text{asy}}V_j[n-k],n>k\end{cases} \tag{21}$$

V. CASE STUDIES

This section presents a comprehensive performance evaluation of the proposed NLA-HEM. To demonstrate its effectiveness, NLA-HEM is benchmarked against two established methods: the conventional Newton-Raphson (NR) method and the C-HME method. The comparison is conducted across a series of power systems of varying scales, from the standard 39-bus to the large-scale 6468-bus system.

A. In mid-size system simulation

As observed in Fig. 3, the convergence curves of NLA-HEM closely mirror those of C-HME at both 39 and 300 buses system. This close alignment indicates that the two methods possess virtually indistinguishable convergence speeds. The results of two method are almost the same.

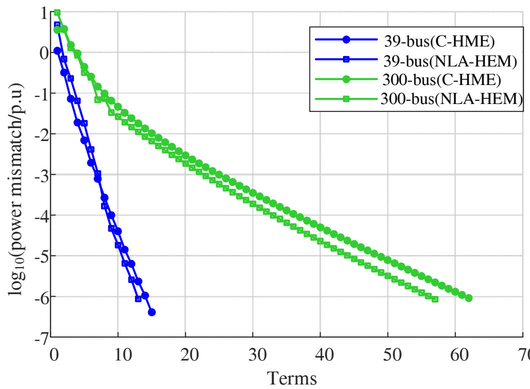

Fig. 3. Maximum power mismatch of NLA-HEM (with parameter K=2) and C-HEM in 39 and 300-bus system.

B. In larger scale system 1888-bus system

To evaluate the performance of the proposed method, a case study was carried out on an 1888-bus system. This system is known to cause divergence in the C-HEM and fails to converge under a flat start in the NR method.

As illustrated in Fig. 4, both the C-HEM and NR methods diverged as the recursion terms increased. In contrast, the proposed NLA-HEM method consistently reduced the power mismatch, eventually converging below the threshold of 10^{-6}. This result confirms the superior convergence robustness of the proposed approach in large-scale power systems.

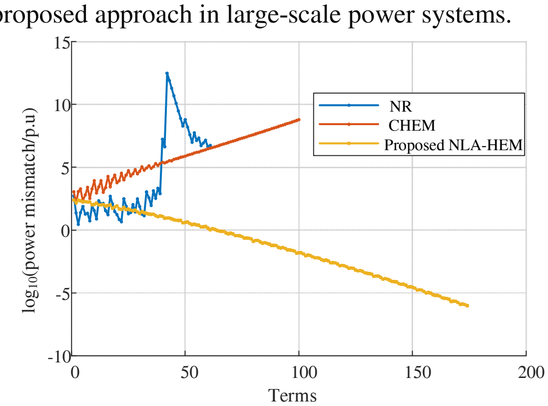

Fig. 4. Maximum power mismatch in 1888-bus system.

In addition, the time cost on 1888-bus system is given in Table I. The solution time of our method varies with the parameter K, as it directly affects the number of terms required for convergence. As noted in the table, compared to NR with its default initial values, our method is computationally slower.

Table I Comparison of time cost on 1888-bus system

Method	Settings	convergence	iterations	time/ms
NR	flat start	×	10	36
	default value	√	2	151
C-HEM	flat start	×	200	1116
NLA-HEM	flat start(K=2)	√	174	716
	flat start(K=3)	√	121	406
	flat start(K=5)	√	132	450
	flat start(K=8)	√	204	921

C. Impact of the Key Parameter K

Equations (8)-(9) indicates that the hyper-parameter K influences the embedding rate of asymmetrical part of the admittance matrix. To analyze its impact on convergence behavior, tests were conducted on the 1888-bus system. As shown in Fig. 5, the convergence curves are compared for K = 2, 3, 4, 5, 8, 10, and 20 in the 1888-bus system.

The results reveal that the convergence speed is highly sensitive to the value of K. The fastest convergence is achieved at K = 3 and 4, whereas slower convergence is observed both at a smaller value (K=2) and larger values (K≥ 5). These findings underscore that selecting an appropriate value for K is critical to the performance of the proposed NLA-HEM. For practical, we recommend choosing K between 4 and 10. This range serves as a practical guideline, though the best value may vary by system.

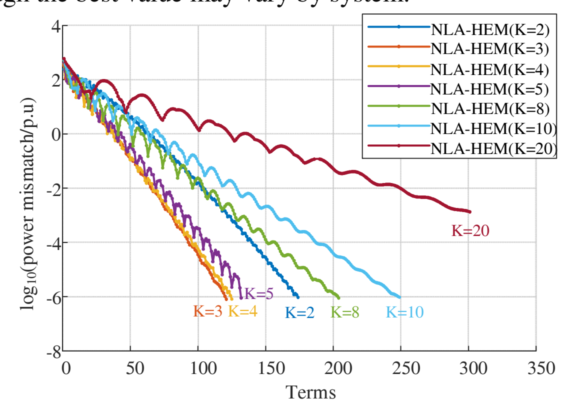

Fig. 5. Convergence performance with varying parameter K in 1888-bus system.

D. Detection of Convergence Issues

A distinctive advantage of the proposed NLA-HEM framework lies in its inherent capability to detect and preempt potential convergence failures, a feature not readily available in traditional methods like the NR. Traditional solvers often diverge abruptly without providing diagnostic information on the failure mechanism. In contrast, the progression of the power mismatch through the embedding stages in our method serves as a indicator of solution path stability.

As illustrated in Fig. 6 for the 6468-bus system, the divergence of the conventional C-HEM and NR methods is immediate and offers no recourse for mid-process correction.

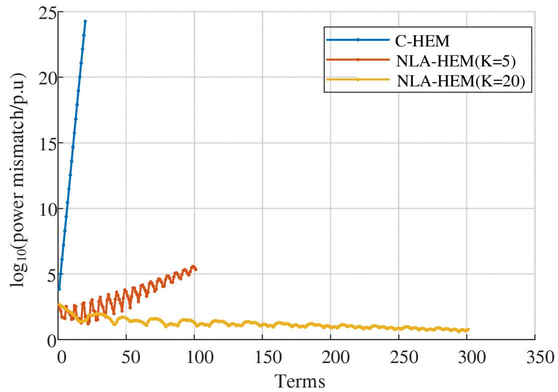

Fig. 6. Convergence performance of different methods in 6468-bus system.

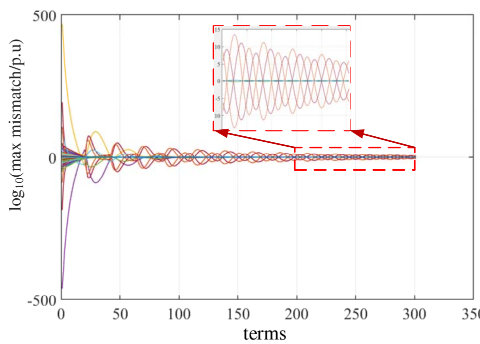

Fig. 7. Convergence performance with parameter K=20 in 6468-bus system.

As shown in Fig. 7, the mismatch becomes very low, but it continues to oscillate. The power mismatch oscillations were observed at buses 1501, 3598, 4272, and 4293. To mitigate this issue and improve convergence, the reactance values of the branches connecting these buses—which originally exhibited large phase-shift angles—were increased to ten times their original values[12].

After the adjustment, the resulting power mismatch curve is given in Fig. 8, which shows the proposed NLA-HEM successfully converging under the modified configuration. This confirms the advantage of the proposed holomorphic embedding formulation in detecting and resolving convergence issues in challenging power system networks.

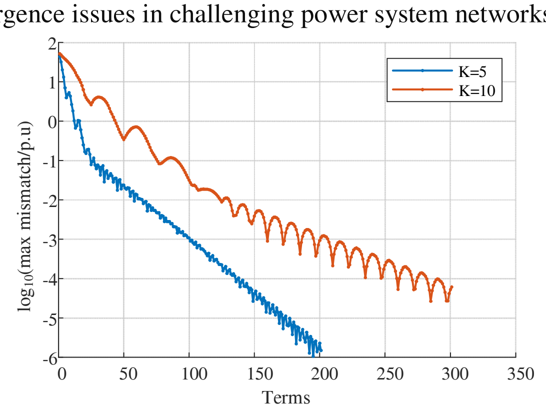

Fig. 8. Convergence performance in 6468-bus system after adjust.

VI. Conclusion

This paper has proposed a novel holomorphic embedding power flow method based on a nonlinear admittance embedding formulation. The core of the approach lies in the designed embedding structure for the admittance matrix and the corresponding numerical procedure for efficiently solving the resulting coefficients.

Simulation results on the 1888-bus system, as shown in Fig. 4 and Fig. 5, demonstrate that the proposed method achieves superior convergence performance compared to C-HEM. Moreover, it exhibits an inherent capability to detect potential convergence issues, offering valuable diagnostic insight during the solution process.

This work also provides a diagnosable tool for large-scale power flow analysis, especially in ill-conditioned systems where conventional methods may fail.

References

[1] W. F. Tinney, C. E. Hart, "Power flow solution by Newton's method," IEEE Trans. Power Appar. Syst., no. 11, pp. 1449-1460, 2007.

[2] A. Trias, "The holomorphic embedding load flow method," IEEE Power Energy Soc. Gen. Meeting, San Diego, CA, USA, pp. 1-8, 2012.

[3] M. Heidarifar, P. Andrianesis and M. Caramanis, "Holomorphic embedding load flow method in three-phase distribution networks with ZIP loads," IEEE Trans. Power Syst., vol. 38, no. 5, pp. 4605-4616, 2023.

[4] Y. Zhao, C. Li, T. Ding, Z. Hao, F. Li, "Holomorphic embedding power flow for AC/DC hybrid power systems using Bauer's Eta algorithm," IEEE Trans. Power Syst. vol. 36, no. 4, pp. 3595-3606, 2021.

[5] C. Liu, K. Sun, B. Wang, W. Ju, "Probabilistic power flow analysis using multi-dimensional holomorphic embedding and generalized cumulants," IEEE Trans. Power Syst., vol. 33, no. 6, pp. 7132-7142, 2018.

[6] Q. Lai, C. Liu, and K. Sun, "Analytical static voltage stability boundary based on holomorphic embedding," Int. J. Electr. Power Energy Syst., vol. 134, 2022.

[7] Q. Lai, C. Liu, and K. Sun, "Vulnerability assessment for voltage stability based on solvability regions of decoupled power flow equations," Appl. Energy, vol. 304, 2021.

[8] R. D. Zimmerman, C. E. Murillo-Sánchez and R. J. Thomas, "MATPOWER: Steady-State Operations, Planning, and Analysis Tools for Power Systems Research and Education," IEEE Trans. Power Syst., vol. 26, no. 1, pp. 12-19, Feb. 2011.

[9] F. D. Freitas, A. C. Santos, L. F. J. Fernandes, Y. G.I. Acle, "Restarted holomorphic embedding load-flow model based on low-order Padé approximant and estimated bus power injection," Int. J. Electr. Power Energy Syst., vol. 112, 2019, 326-338.

[10] H. D. Chiang, T. Wang and H. Sheng, "A novel fast and flexible holomorphic embedding power flow method," IEEE Trans. Power Syst., vol. 33, no. 3, pp. 2551-2562, May 2018.

[11] S. Rao, Y. Feng, D. J. Tylavsky and M. K. Subramanian, "The holomorphic embedding method applied to the power-flow problem," IEEE Trans. Power Syst., vol. 31, no. 5, pp. 3816-3828, Sept. 2016.

[12] Y. Luo, C. Liu and K. Sun, "An improved holomorphic embedding method for power flows with phase-shifting transformers," CSEE J. Power Energy Syst., early access, Jan. 07, 2026, doi: 10.17775/CSEEJPES.2024.07680.

979-8-3315-8138-1

979-8-3315-8138-1